Research Article

Numerical analysis of coupled fluid flow and natural heat transfer on a vertical flat plate

Mehdi GHAMATI[1] , **Nematollah ASKARI[1]** , **Morteza ABBASI[2]** , **Seyed Morteza MOGHIMI[3]** ,
Seyed Masoud KHODADI[1] , **Mohammad Hasan TAHERI[1,*]**

[1]*Department of Mechanical Engineering, Faculty of Imam Khomeini, Behshahr Branch, Technical and Vocational University (TVU), Mazandaran, 1435661137, Iran*
[2]*Department of Mechanical Engineering, Sari Branch, Islamic Azad University, Sari, 1477893855, Iran*
[3]*Department of Mechanical Engineering, Qaemshahr Branch, Islamic Azad University, Qaemshahr, 4765161964, Iran*

ARTICLE INFO

ABSTRACT

This study aims to look into the temperature distribution on a vertical flat plate with a variable temperature boundary condition. As a novelty, the variable temperature is considered on the wall, and coupled momentum and energy equation are solved. Moreover, a novel variable change transforms the infinite boundary condition into the finite one. The partial differential governing equations were introduced and transformed into ordinary differential equations form using the similarity solution. The obtained equations were numerically solved and validated using previous research. The results showed that for a constant variable temperature index (n), increasing the Prandtl number (Pr) from 0.1 to 2 reduces the dimensionless maximum velocity by less than half and the skin friction coefficient by about 32%. In this case, the dimensionless temperature approaches zero faster; as a result, the thermal boundary layer thickness declines, and the Nusselt number (Nu) rises. Furthermore, for a constant Pr, when n increases from 0 to 1.5, the dimensionless maximum velocity and the skin friction decrease by about 38% and 23%, respectively. Since the dimensionless temperature continues to descending trend, Nu still rises in this case.

Cite this article as: Ghamati M, Askari N, Abbasi M, Moghimi SM, Khodadi SM, Taheri MH. Numerical analysis of coupled fluid flow and natural heat transfer on a vertical flat plate. J Ther Eng 2024;10(1):1–9.

INTRODUCTION

The investigation of boundary layer flow behavior over vertical plates is important because of its application in thermal industries and facilities such as heat exchangers [1,2], heat pipes [3], electronic equipment [4,5], and vertical fin [6-8]. Furthermore, many thermal facilities expose themselves to free fluid flows and exchange heat. In the free convection process, the density difference creates a buoyancy force, which drives the fluid to move. Natural convection is the predominant heat transfer mechanism,

and the buoyancy force significantly impacts the boundary layer fluid flow in this heat transfer process. However, the lower heat transfer rate is the main problem of natural convection systems compared to forced convection systems. Several solutions have been suggested to compensate for this problem, such as increasing the insulation area or using variable temperatures on the wall.

Chakkingal et al. [9] researched free convection and conjugate heat transfer in a simple cubic packing design using a numerical simulation. This study examined the influence of non-uniform wall temperature on fluid flow and local heat transfer for various Rayleigh (Ra) and Prandtl (Pr) numbers. Compared to the uniform temperature on the wall, spatial variation in wall temperature resulted in a significant improvement in heat transfer for the same mean temperature difference. Furthermore, compared to uniform wall temperatures, using a spatial variation in wall temperature at a well-chosen phase angle can result in significant heat transfer enhancement. Nonetheless, this reaches the expense of rising entropy generation.

Sompong and Witayangkurn [10] analyzed the performance of wavy geometry on free convection heat transfer. They considered a porous media-filled enclosure with two vertical wavy walls. The problem was solved using the finite element method (FEM). A set of effective parameters was selected (the values of wave amplitude ($\lambda = 0.05$ and 0.1) and the number of undulations (n = 1 and 2) are chosen with constants Ra = 10^5, Da = 10^{-3}, and Pr = 0.71), and their impact was explored. Increases in wave number do not affect free convective heat transfer in an enclosure.

Javaherdeh et al. [11] numerically presented a study on a two-dimensional laminar natural convection heat transfer with moving vertical plates in a porous medium considering the magnetic field. They evaluated dimensionless velocity, thermal, and concentration profiles, as well as presented numerical data for local Nusselt and Sherwood numbers. They reported that increases in the wall temperature power law index (n) are associated with decreases in fluid velocity and temperature. The more significant the temperature difference between the moving plate and the fluid, the greater the Nusselt number.

The effects of time-periodic boundary conditions on natural convection heat and mass transfer in a vertical cylindrical porous channel were probed by Mohammed and Giddings [12]. They demonstrated that the aspect ratio significantly impacts Nusselt and Rayleigh's numbers. Increasing the Rayleigh number causes an increase in convective velocity, which affects the position of the hot region and reduces the temperature field. When the aspect ratio is increased, a warm stream forms in the center of the cylinder. As the heating period increases, the circulation becomes faster, and the intensity of the temperature contour layers decreases. A correlation for Nu as a function of the parameters mentioned above is developed in this work.

Feng Wu and Gang Wan [13] numerically simulated natural convection in an inclined porous cavity with a partially active thermal sidewall under time-periodic boundary conditions. They discovered that a partial active thermal boundary condition on one wall could result in heat transfer on the opposing walls. Furthermore, compared to uniform temperature distribution, the results showed that non-uniform uniform temperature distribution reduces the oscillation amplitude of the Nusselt number on a wall. The numerical and experimental study of convective heat transfer in a vertical porous channel was carried out by Foudhil et al. [14] utilizing a non-equilibrium model. Their findings revealed that increasing the Biot number improved heat transfer between the heated wall and the porous domain. The influence of particle thermal conductivity on heat transfer in the porous medium decreases as the thermal conductivity of the metallic beads increases, particularly as the diameter of the beads increases. Nusselt numbers based on particle diameter are related to Reynolds numbers and particle diameter.

Abo-Eldahab and El Aziz [15] discussed the natural heat transfer of a Newtonian fluid flow over a vertical plate with variable temperature. The governing equations for viscous dissipation, Joule heating, thermal source, and magnetic field were numerically solved. According to the findings, increasing the magnetic field reduces the dimensionless velocity component while increasing the dimensionless temperature. Pantokratoras [16] and Aydin and Kaya [17] reviewed the impact of viscous dissipation on natural convection heat transfer on a vertical plate. The interaction between viscous dissipation and buoyancy force, as well as temperature distribution, was investigated. In another study, Aydin and Kaya [18] probed the hydromagnetic mixed heat transfer on a permeable vertical plate while considering viscous dissipation and ohmic heat. They discovered that either Richardson number augmentation or Eckert number reduction could augment the local heat transfer coefficient and skin friction coefficient. Mamun et al. [19] and Palani et al. [20] examined the effect of viscous dissipation and heat source on a vertical flat plate. A natural heat transfer on magnetohydrodynamics (MHD) fluid flow was considered, and both researchers solved the problem numerically. Desale and Pradhan [21] considered a flat plate with variable wall temperature and viscous dissipation. A similar solution was applied, and the ordinary differential equations (ODEs) were solved by the numerical finite difference method (FDM). They reported with the increase of Eckert number, temperature increases but heat transfer rate reduces on the wall. Reddy and Machireddy [22] presented a study on the impact of thermal radiation, viscous dissipation, and Hall current on MHD convection flow over a stretched vertical flat plate. They used 4th-order Runge-Kuta (RK4) for solving the governing equations. The effect of critical parameters, including viscous dissipation, thermal radiation, and buoyancy, was analyzed on the velocity and temperature profiles. The results showed that viscous dissipation and thermal radiation could increase the velocity and

temperature. Al-Odat and Al-Azab [23] examined how a magnetic field affects natural convection heat transfer with a conducting fluid flow over a vertical plate in addition to considering chemical reactions. They numerically analyzed the problem and investigated the impact of various parameters. It was concluded that when chemical reaction parameters were reduced, both velocity and concentration decreased. The magnetic parameter, on the other hand, only reduces velocity. Makinde [24] investigated a magnetic boundary layer fluid flow with heat and mass transfer over a vertical plate numerically as well. Natural convection in a differentially heated wavy cavity under thermophoresis was studied by Grasan et al. [25] and Sheremet [26]. The governing equations were numerically solved after being mathematically modeled.

A numerical investigation of the natural convection over a vertical wall with constant flux between 400 to 660 W/m^2 was published by Yildiz and Basaran [27]. They showed that with the increase of heat flux on the wall, the wall temperature increased. Consequently, the air velocity in the boundary layer increased. So, an increase in the air near the wall was observed.

Acharya [28] explored a study on the flow pattern and heat transfer of nanofluid natural convection in square, circular and hexagonal enclosures. The research outcomes revealed that by variation of Rayleigh number from 10^3 to 10^5, Hartmann number between 5 to 15, and nanofluid concentration up to 0.04, the heat transfer rate in circular obstacles increases about 28 %. However, less heat transfer rate was reported for hexagonal obstacles.

Recently, investigation on the heat transfer by natural convection has been published, such as Akinshilo [29], Ekiciler [30], Rao et al. [31], Taskesen et al. [32], Rana et al. [33].

Considering the above literature review, the investigation of natural heat transfer on vertical plates is an interesting field of scientific research. As a boundary condition on the plate, most research considers either a constant wall temperature or a constant heat flux. In fact, it is ideal to assume a constant temperature or heat flux on a wall when studying the heat transfer process on a vertical plate. Plates experience temperature variations in real and applicable cases, and the constant temperature or heat flux is improper. As a result, the research aims to explore natural heat transfer and fluid flow over a vertical plate with variable temperatures on the wall. As a novelty, a variable boundary condition on the wall is applied. Further, a new variable change is applied to transform the infinite boundary condition into a finite condition. The nondimensional coupled momentum and energy equations obtained via similarity solution are solved numerically using Runge-Kutta 4th order. The impact of various parameters is analyzed on fluid flow and natural heat transfer characteristics on a wall.
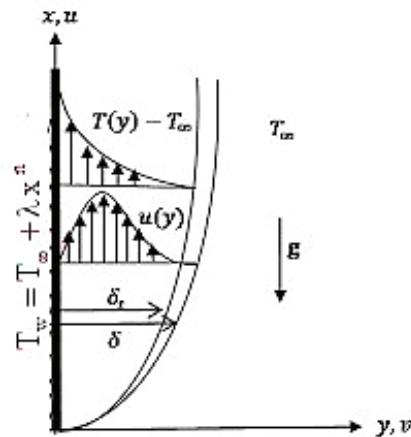
Figure 1. Schematic of problem [34].

DESCRIPTION OF THE PROBLEM

The boundary layer fluid flow and natural convection heat transfer along with a vertical plate are investigated. Figure 1 presents a graphic illustration of the problem:

The plate is depicted in Cartesian coordinates. The x-axis denotes the vertical axis, and the y-axis represents the horizontal axis. The terms u and v are defined as velocity components along with the x and y axes, respectively.

As shown in Figure 1, a variable temperature boundary condition ($T_w = T_\infty + \lambda x_n$) is selected for a wall temperature with a constant coefficient, and n is a variable temperature index.

The following are the definitions of the governing equations, which include continuity, momentum, and energy equations [34]:

$$\nabla \cdot \vec{V} = 0 \tag{1}$$

$$\rho \frac{D\vec{V}}{Dt} = -\nabla P + \mu_f \nabla^2 \vec{V} \tag{2}$$

$$\rho c_p \frac{DT}{Dt} = -k \nabla^2 T \tag{3}$$

Where V, P, T, μ_f, ρ, c_p, t, and k are the velocity field, the pressure, the temperature, the dynamic viscosity, the density, specific thermal capacity, the time, and the thermal conductivity, respectively. Equations (1-3) can be rewritten for our two-dimensional problem as [34]:

$$\frac{\partial u_{(x,y)}}{\partial x} + \frac{\partial v_{(x,y)}}{\partial y} = 0 \tag{4}$$

$$u_{(x,y)} \frac{\partial u_{(x,y)}}{\partial x} + v_{(x,y)} \frac{\partial u_{(x,y)}}{\partial y} = g\beta(T - T_\infty) + \nu \frac{\partial^2 u_{(x,y)}}{\partial y^2} \tag{5}$$

$$u_{(x,y)}\frac{\partial T}{\partial x}+v_{(x,y)}\frac{\partial T}{\partial y}=\alpha\frac{\partial^2 T}{\partial y^2} \qquad (6)$$

Where υ, g, β, T, T_∞, and α are kinematic viscosity, gravity, thermal expansion coefficient, temperature field, ambient temperature, and thermal diffusivity coefficient, respectively.

Besides, the boundary conditions are defined as:

$$y=0 \quad \rightarrow \quad u=v=0 \text{ and } T=T_w \qquad (7a)$$

$$y\rightarrow\infty \quad \rightarrow \quad u=v=0 \text{ and } T=T_\infty \qquad (7b)$$

Where T_w is the temperature of plate.

MATHEMATICAL DISCRIPTION

Similarity Solution

Solving the governing equations requires converting the equations into ODEs. With the variable temperature assumption [35] on the wall and defining a dimensionless parameter (η), the remaining parameters are introduced in dimensionless form as follows [35]:

$$\eta=(\frac{Gr_{(x)}}{4})^{\frac{1}{4}}\frac{y}{x} \qquad (8a)$$

$$u_{(x,y)}=2\sqrt{x\beta g(T_w-T_\infty)}\,f'_{(\eta)}=2\sqrt{\beta g\lambda x^{n+1}}\,f'_{(\eta)} \qquad (8b)$$

$$Gr_{(x)}=\frac{\beta g(T_w-T_\infty)x^3}{\nu^2} \qquad (8c)$$

$$\theta=\frac{T-T_\infty}{T_w-T_\infty} \qquad (8d)$$

Where $f'_{(\eta)}$, $Gr_{(x)}$ and $\theta_{(\eta)}$ are the dimensionless velocity, Grashof number, and dimensionless temperature, respectively.

By defining c=βgλ, we have [34]:

$$\frac{\partial\eta}{\partial x}=\frac{1}{\sqrt{2}}\frac{n-1}{4}\frac{c^{\frac{1}{4}}x^{\frac{n-5}{4}}}{\nu^{\frac{1}{2}}}y \qquad (9a)$$

$$\frac{\partial\eta}{\partial y}=\frac{1}{\sqrt{2}}\frac{c^{\frac{1}{4}}x^{\frac{n-1}{4}}}{\nu^{\frac{1}{2}}} \qquad (9b)$$

Also, according Equation (1), $v_{(x,y)}$ can be rewritten:

$$v_{(x,y)}=-\frac{\partial}{\partial x}(\int_0^y u_{(x,y)}dy)=-\frac{\partial}{\partial x}\int_0^1 2c^{\frac{1}{2}}x^{\frac{n+1}{2}}f'_{(\eta)}\sqrt{2}\nu^{\frac{1}{2}}c^{-\frac{1}{4}}x^{\frac{n-1}{4}}d\eta$$

$$=-\sqrt{2}\frac{n+3}{2}c^{\frac{1}{4}}\nu^{\frac{1}{2}}x^{\frac{n-1}{4}}f_{(\eta)}-\frac{n-1}{2}c^{\frac{1}{2}}x^{\frac{2n-2}{4}}yf'_{(\eta)} \qquad (10)$$

Now, the other velocity differentiation can be computed as follows:

$$\frac{\partial u_{(x,y)}}{\partial x}=2c^{\frac{1}{2}}\frac{\partial}{\partial x}(x^{\frac{n+1}{2}}f'_{(\eta)})=[(n+1)c^{\frac{1}{2}}x^{\frac{n-1}{2}}f'_{(\eta)}+\frac{1}{\sqrt{2}}\frac{n-1}{2}\frac{1}{\nu^{\frac{1}{2}}}c^{\frac{3}{4}}x^{\frac{3n-3}{4}}yf''_{(\eta)}] \qquad (11a)$$

$$\frac{\partial u_{(x,y)}}{\partial y}=\frac{\partial u_{(x,y)}}{\partial\eta}\times\frac{\partial\eta}{\partial y}=2c^{\frac{1}{2}}x^{\frac{n+1}{2}}f''_{(\eta)}\times\frac{1}{\sqrt{2}}\frac{c^{\frac{1}{4}}x^{\frac{n-1}{4}}}{\nu^{\frac{1}{2}}}=\frac{2}{\sqrt{2}}\frac{c^{\frac{3}{4}}x^{\frac{3n+1}{4}}}{\nu^{\frac{1}{2}}}f''_{(\eta)} \qquad (11b)$$

$$\frac{\partial^2 u_{(x,y)}}{\partial y^2}=\frac{\partial}{\partial y}(\frac{\partial u_{(x,y)}}{\partial y})=\frac{2}{\sqrt{2}}\frac{c^{\frac{3}{4}}x^{\frac{3n+1}{4}}}{\nu^{\frac{1}{2}}}\times\frac{1}{\sqrt{2}}\frac{c^{\frac{1}{4}}x^{\frac{n-1}{4}}}{\nu^{\frac{1}{2}}}f'''_{(\eta)}=\frac{cx^n}{\nu}f'''_{(\eta)} \qquad (11c)$$

Substituting Equations (8)-(11) into Equation (5), the ODE form of momentum equations can be obtained as:

$$f'''_{(\eta)}+(n+3)f_{(\eta)}f''_{(\eta)}-2(n+1)f'^2_{(\eta)}+\theta_{(\eta)}=0 \qquad (12)$$

The temperature differentiations also are calculated as follows:

$$\frac{\partial T}{\partial x}=\frac{\partial}{\partial x}(T_\infty+\lambda x^n\theta_{(\eta)})=n\lambda x^{n-1}\theta_{(\eta)}+\frac{1}{\sqrt{2}}\frac{n-1}{4}\lambda c^{\frac{1}{4}}\frac{1}{\nu^{\frac{1}{2}}}yx^{\frac{5n-5}{4}}\theta'_{(\eta)} \qquad (13a)$$

$$\frac{\partial T}{\partial y}=\frac{\partial}{\partial y}(T_\infty+\lambda x^n\theta_{(\eta)})=\lambda x^n\frac{\partial\theta_{(\eta)}}{\partial\eta}\frac{\partial\eta}{\partial y}=\frac{1}{\sqrt{2}}\lambda c^{\frac{1}{4}}\frac{1}{\nu^{\frac{1}{2}}}x^{\frac{5n-1}{4}}\theta'_{(\eta)} \qquad (13b)$$

$$\frac{\partial^2 T}{\partial y^2}=\frac{\partial}{\partial y}(\frac{\partial T}{\partial y})=\frac{\partial}{\partial y}(\frac{1}{\sqrt{2}}\lambda c^{\frac{1}{4}}\frac{1}{\nu^{\frac{1}{2}}}x^{\frac{5n-1}{4}}\theta'_{(\eta)})=\frac{1}{2}\lambda c^{\frac{1}{2}}\frac{1}{\nu}x^{\frac{6n-2}{4}}\theta''_{(\eta)} \qquad (13c)$$

Inserting Equation (13) into the Equation (6) and some simplification, the ODE form of energy equations is achieved:

$$\theta''_{(\eta)}+(n+3)Pr f_{(\eta)}\theta'_{(\eta)}-4n Pr f'_{(\eta)}\theta_{(\eta)}=0 \qquad (14)$$

Where Pr is the Prandtl number, the Nusselt number is defined as [34]:

$$Nu_x=\frac{h\,y}{K}=\frac{q_w}{k\frac{(T_w-T_\infty)}{y}}=-\frac{(\frac{\partial T}{\partial y})_{y=0}\,y}{(T_w-T_\infty)} \qquad (15)$$

Where h is the thermal convection coefficient, now by using Equation (13b), Nu_x can be rewritten as:

$$Nu_x=-\frac{1}{\sqrt{2}}c^{\frac{1}{4}}\frac{1}{\nu^{\frac{1}{2}}}x^{\frac{n-1}{4}}\frac{x}{x}\theta'_{(0)}y=-\frac{1}{\sqrt{2}}c^{\frac{1}{4}}x^{\frac{n+3}{4}}\frac{1}{\nu^{\frac{1}{2}}}\theta'_{(0)}\frac{y}{x}=-\eta\theta'_{(0)} \qquad (16)$$

Additionally, by converting the boundary conditions into the dimensionless form, we can obtain the following:

$$\eta=0 \quad \rightarrow \quad f(0)=f'(0)=0 \qquad \theta(0)=1 \qquad (17a)$$

$$\eta=\infty \quad \rightarrow \quad f'(\infty)=0 \qquad \theta(\infty)=0 \qquad (17b)$$

Solution Methodology

The dimensionless form of momentum and energy equations are coupled, as shown in Equation (12) and Equation (14). As a result, they must solve the problem simultaneously. A Maple code was used in this study, and coupled equations were solved numerically with the Runge-Kutta method 4th order (RK4).

Fourth-order Runge-Kutta

Runge-Kutta methods are iterative methods used in numerical analysis. A powerful tool for solving ordinary differential equations is the Rung-Kutta method. The most well-known is Runge-Kutta's classic method, also known as the fourth-order Runge-Kutta method.

By considering the following equation:

$$\frac{dx}{dy} = f(x, y), \; y(0) = y_0 \tag{18}$$

It is needed to determine the value of the unknown function y at the point x. The Runge-Kutta method approximates the value of y for a given x as follows:

$$
\begin{aligned}
k_1 &= hf(x_n, y_n) \\
k_2 &= hf(x_n + \frac{h}{2}, y_n + \frac{k_1}{2}) \\
k_3 &= hf(x_n + \frac{h}{2}, y_n + \frac{k_2}{2}) \\
k_3 &= hf(x_n + \frac{h}{2}, y_n + k_3) \\
y_{n+1} &= y_n + k_1/6 + k_2/3 + k_3/3 + k_4/6 + O(h^5)
\end{aligned}
\tag{19}
$$

Where h is the length of each step and y_{n+1} is the approximation of RK4.

Validation

Due to the novelty of our work and the lack of similar results in the literature, we chose to compare the results with previous studies in a special case to validate the accuracy of the RK4 outcomes. As shown in Figures 2a and 2b, our numerical results were compared to the Ref. [34] results for n=0. The results can be seen to be overlapping. Furthermore, the skin friction coefficient directly correlates with the velocity rate (f') and the Nusselt number with the dimensionless temperature rate (θ'). Table 1 compares our results to the results of Ref. [34] for the constant temperature on the wall. The results were found to be satisfactory.

Table 1. The present study results are compared with those of Ref [34] - f''(η) and θ'(η) and various Pr

Pr	f''(0)	f''(0)[34]	θ'(0)	θ'(0)[34]
0.01	0.9873	0.9873	0.0807	0.0807
0.1	0.8592	0.8591	0.2302	0.2301
0.72	0.676	0.676	0.5046	0.5046
1	0.6422	0.6422	0.5671	0.5671
2	0.5713	0.5713	0.7165	0.7165
3	0.5309	0.5309	0.8155	0.8155
6	0.4648	0.4649	1.007	1.007
10	0.4192	0.4192	1.169	1.169
30	0.3311	0.3312	1.589	1.589
100	0.2517	0.2517	2.191	2.191
1000	0.1449	0.1449	3.964	3.965

(a)

(b)
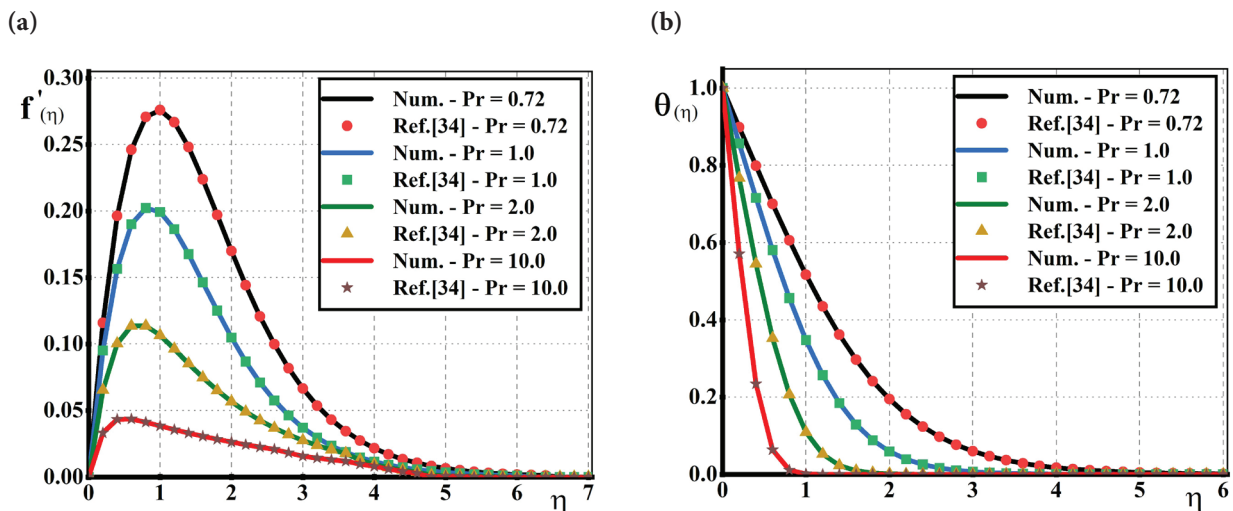
Figure 2. The present study's results are compared with those in Ref [34]- (a) f'(η) and (b) θ(η)

RESULTS AND DISCUSSION

This section reviews and analyses the findings. Figures 3a and 3b show the effects of Pr on the f'(η) and $\theta(\eta)$ profiles for n=1. Temperature changes alter the velocity distribution because momentum and energy equations are coupled. With increasing Pr, the maximum velocity value decreases and reaches the boundary layer outside velocity faster (zero velocity) as shown in Figure 3a. For the same Pr, the maximum velocity value decreases for Figure 2a (n=0), indicating that the maximum velocity value decreases as n increases. Due to an increase in Pr, the kinematic viscosity increases. Therefore, the resistive force against the flow increases, resulting in a reduction in velocity.

According to Figure 3b, the dimensionless temperature tends to zero faster as Pr increases. The fluid flow temperature reaches the wall temperature according to the dimensionless temperature definition. As Pr increases, the thermal domination decreases; therefore, the thermal conductivity decreases. However, the Nu value increases, which

draws the fluid temperature closer to the wall temperature earlier. Based on Equation (8b), the dimensional temperature becomes zero. Unlike Figure 2b for n=0, a higher n causes the temperature to reach the wall temperature later.

f'(η) and $\theta(\eta)$ are influenced by n in Figures 4a and 4b (for Pr=0.72). As n increases, the velocity profile's maximum value decreases (Figure 4a). Figure 4b shows the temperature diagram's slope rising to the wall temperature. As n increases, the difference between wall temperature and free fluid flow temperature increases, increasing convective heat transfer. Due to this, the dimensionless temperature becomes zero more quickly than the fluid temperature reaches the wall temperature. Furthermore, the buoyancy force falls, which reduces velocity.

Figures 5a and 5b illustrate the impact of Pr on Nu and the skin friction coefficient (f"(0)). When Pr grows, the kinematic viscosity increases and f"(0) decreases (Figure 5a). Additionally, as Pr increases, Nu rises, and the heat transfer rate increases (Figure 5b). The Nu value increases when the thermal domination decreases; therefore, the thermal conductivity
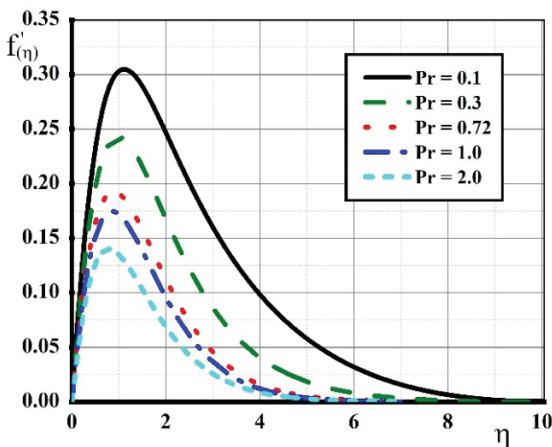
Figure 3a. Variation of Pr with f'(η) (n=1)
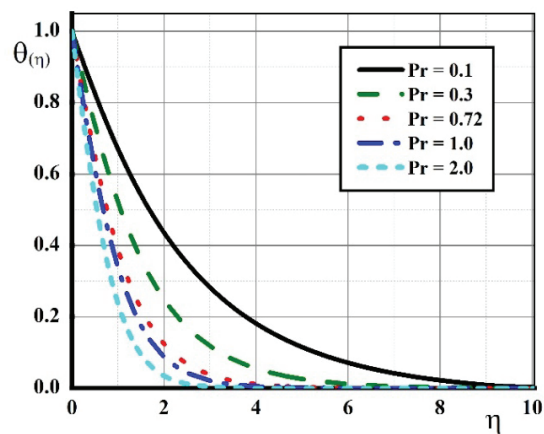
Figure 3b. Variation of Pr with $\theta(\eta)$ (n=1)
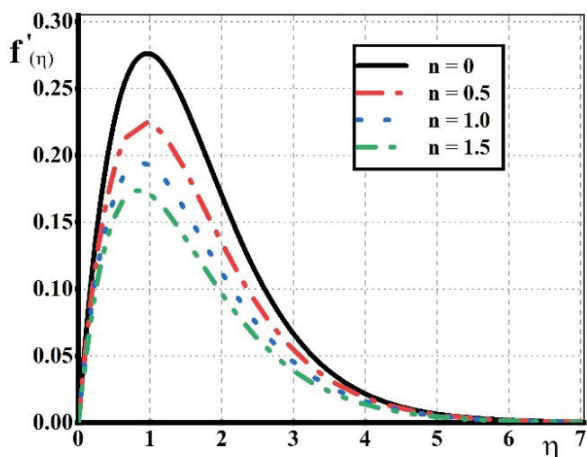
Figure 4a. Examination of n change on f'(η) at Pr=0.72
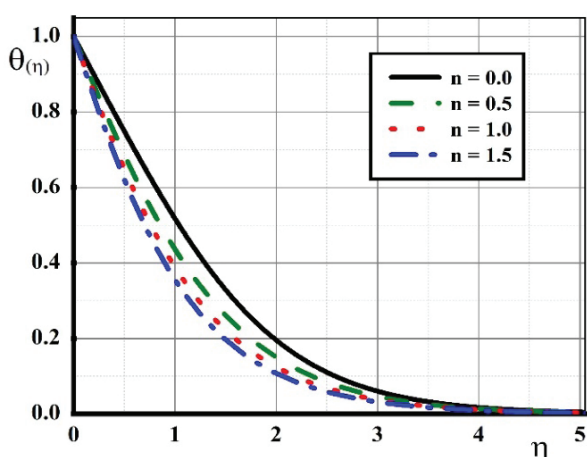
Figure 4b. Examination of n change on $\theta(\eta)$ for Pr=0.72
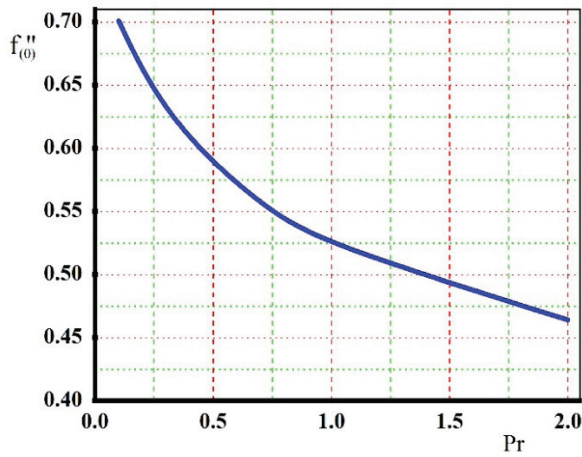
Figure 5a. For n =1, the effect of Pr on f"(0)
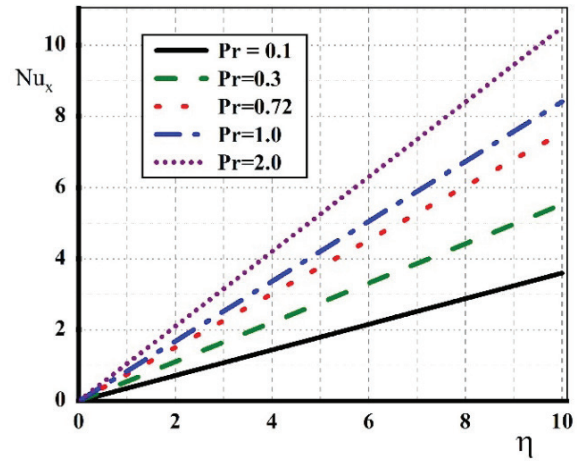
Figure 5b. For n=1, the effect of Pr on Nu_x
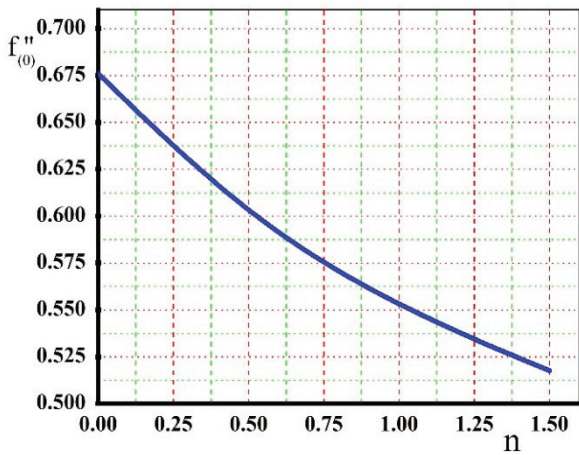
Figure 6a. Influence of n on f"(0) (skin friction coefficient) for Pr=0.72
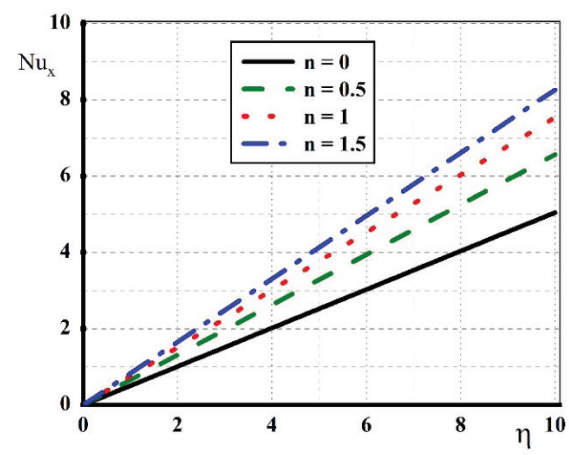
Figure 6b. Influence of n on Nu_x for Pr=0.72
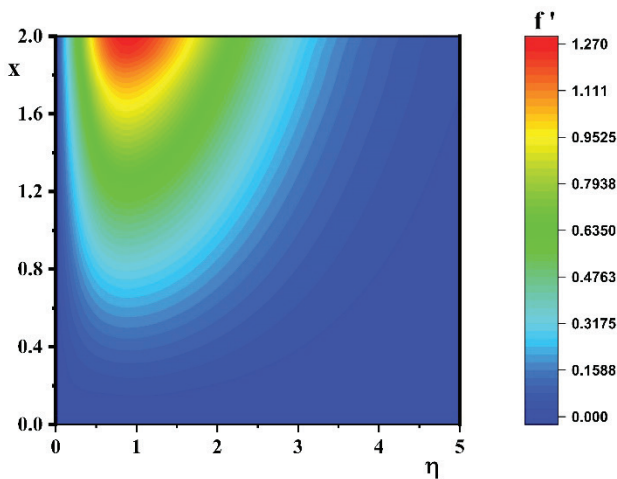
Figure 7a. Contour of dimensionless velocity (f') for n=0.5, Pr=0.72
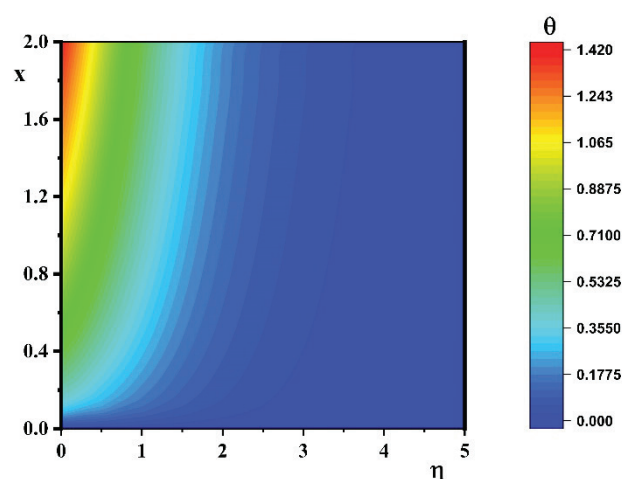
Figure 7b. Contour of dimensionless temperature (θ) for n=0.5, Pr=0.72

decreases; however, when the Nu value increases, the fluid temperature reaches the wall temperature more quickly.

Figures 6a and 6b illustrate how n affects f"(0) and Nu. As n increases, f"(0) decreases (Figure 6a). Figure 6b further demonstrates that Nu increases with increasing n, accelerating the rate of heat transfer. It occurs because convective heat transfer rises.

For capturing better physical comprehension, the contour of dimensionless velocity and temperature for n=0.5 and Pr=0.72 is illustrated in Figure 7.

CONCLUSION

The partial differential equations in this study were converted into ordinary differential equations using similarity solutions. The variable temperature boundary condition was chosen for the wall as a novelty. Also, by applying a new variable change, an infinite boundary condition was transformed into the finite one. The coupled momentum and energy equations were numerically solved. The following deductions were made:

- The maximum value of dimensionless velocity (f'_{max}) decreases 40-50 % as Pr rises. The velocity thus approaches the outside velocity more quickly. In addition, f'_{max} reduces when compared to the boundary condition of constant temperature on the wall.
- It can be concluded that f'_{max} velocity drops between 23 to 38 % as n increases. $\theta(\eta)$ also drops. But the fluid temperature slope rises, and it gets closer to the wall temperature more quickly.
- It can be observed that f"(0) decreases about 20-35 % as Pr rises. This enhances the rate of dimensionless heat transfer.
- A higher n leads to a lower f"(0). Thus, the dimensionless heat transfer rate rises, and f"(0) falls.

NOMENCLATURE

Cp	Specific heat, kJ / kg °C
f	Dimensionless velocity
g	Gravity acceleration, m/s^2
Gr	Grashof number
k	Thermal conductivity, W / m °C
n	Variable temperature index
P	Pressure, Pa
T	Temperature, °C
T_w	Wall temperature, °C
T_∞	Free fluid temperature, °C
u	Vertical velocity, m/s
v	Horizontal velocity, m/s.
V	Velocity field, m/s
x	Vertical axis, m
y	Horizontal axis, m

Greek symbols

β	Thermal expansion coefficient (1/ °C)
μ	Dynamic viscosity, Pa s
θ	Dimensionless temperature
ρ	Density, kg/m^3
η	Nondimensional variable

AUTHORSHIP CONTRIBUTIONS

Authors equally contributed to this work.

DATA AVAILABILITY STATEMENT

The authors confirm that the data that supports the findings of this study are available within the article. Raw data that support the finding of this study are available from the corresponding author, upon reasonable request.

CONFLICT OF INTEREST

The author declared no potential conflicts of interest with respect to the research, authorship, and/or publication of this article.

ETHICS

There are no ethical issues with the publication of this manuscript.

REFERENCES

[1] Unger S, Beyer M, Pietruske H, Szalinski L, Hampel U. Natural convection heat transfer performance of additively manufactured tube bundle heat exchangers with novel fin design. Heat Mass Transf 2021;57:1193−1203. [CrossRef]

[2] Srinivas T, Vinod AV. Natural convection heat transfer using water-based nanofluid in a shell and helical coil heat exchanger. Chem Papers 2021;75:2407−2416. [CrossRef]

[3] Ajith K, Aaron MJ, Pillai AS, I. V. Muthuvijayan Enoch, A. Brusly Solomon, M. Sharifpur, et al. Turbulent magnetohydrodynamic natural convection in a heat pipe-assisted cavity using disk-shaped magnesium ferrite nanoparticles. Appl Nanosci 2022;12:1627−1641. [CrossRef]

[4] Syah R, Davarpanah A, Elveny M, Ramdan D. Natural convection of water and nano-emulsion phase change material inside a square enclosure to cool the electronic components. Int J Energy Res 2022;46:2403−2417. [CrossRef]

[5] Roy NC, Saha LK and Siddiqa S. Electrohydrodynamics and thermal radiation effects on natural convection flow in an enclosed domain. Int Commun Heat Mass Transf 2021;126:105437. [CrossRef]

[6] Roy K, Giri A, Das B. Laminar entry region mixed convection heat transfer from an inclined rectangular fin array. Int J Numer Methods Heat Fluid Flow 2020;30:3283−3305. [CrossRef]

[7] Roy K, Das B. Convective heat transfer from an inclined isothermal fin array: A computational study. Therm Sci Eng Progr 2020;17:100487. [CrossRef]

[8] Roy K, Das B. Influence of property variation on natural convection in an isothermal vertical finned channel: An extended study. J Therm Sci Eng Appl 2020;13. [CrossRef]

[9] Chakkingal M, Kenjereš S, Dadavi IA, Tummers MJ, Kleijn CR. Numerical analysis of natural convection in a differentially heated packed bed with non-uniform wall temperature. Int J Heat Mass Transf 2020;149:119168. [CrossRef]

[10] Sompong P, Witayangkurn S. Numerical study of natural convection in a heated enclosure with two wavy vertical walls using finite element method. J Appl Math 2014;2014:853231. [CrossRef]

[11] Javaherdeh K, Nejad MM and Moslemi M. Natural convection heat and mass transfer in MHD fluid flow past a moving vertical plate with variable surface temperature and concentration in a porous medium. Eng Sci Technol Int J 2015;18:423–431. [CrossRef]

[12] Mohammed HI and Giddings D. Natural convection heat and mass transfer in the vertical cylindrical porous channel under the effects of time-periodic boundary condition. J Heat Transf 2019;141:122503. [CrossRef]

[13] Wu F, Wang G. Numerical simulation of natural convection in an inclined porous cavity under time-periodic boundary conditions with a partially active thermal side wall. RSC Adv 2017;7:17519–17530. [CrossRef]

[14] Foudhil W, Dhifaoui B, Jabrallah SB, Belghith A, Corriou JP. Numerical and experimental study of convective heat transfer in a vertical porous channel using a non-equilibrium model. J Porous Media 2012;15:531–547. [CrossRef]

[15] Abo-Eldahab EM, El Aziz MA. Viscous dissipation and Joule heating effects on MHD-free convection from a vertical plate with power-law variation in surface temperature in the presence of Hall and ion-slip currents. Applied Mathematical Modelling 2005;29:579–595. [CrossRef]

[16] Pantokratoras A. Effect of viscous dissipation in natural convection along a heated vertical plate. Appl Math Model 2005;29:553–564. [CrossRef]

[17] Aydın O, Kaya A. Mixed convection of a viscous dissipating fluid about a vertical flat plate. Appl Math Model 2007;31:843–853. [CrossRef]

[18] Aydın O, Kaya A. MHD mixed convection of a viscous dissipating fluid about a permeable vertical flat plate. Appl Math Model 2009;33:4086–4096. [CrossRef]

[19] Mamun A, Chowdhury Z, Azim M, Molla M. MHD-conjugate heat transfer analysis for a vertical flat plate in presence of viscous dissipation and heat generation. Int Commun Heat Mass Transf 2008;35:1275–1280. [CrossRef]

[20] Palani G, Srikanth U, Kim K-Y. Combined effects of viscous dissipation and MHD on free convection flow past a semi-infinite vertical plate with variable surface temperature in the presence of heat source. J Eng Thermophysics 2017;26:113–124. [CrossRef]

[21] Desale S, Pradhan V. Numerical solution of boundary layer flow equation with viscous dissipation effect along a flat plate with variable temperature. Proced Eng 2015;127:846–853. [CrossRef]

[22] Reddy MG. Influence of thermal radiation, viscous dissipation and hall current on MHD convection flow over a stretched vertical flat plate. Ain Shams Eng J 2014;5:169–175. [CrossRef]

[23] Al-Odat M, Al-Azab T. Influence of chemical reaction on transient MHD free convection over a moving vertical plate. Emirates J Eng Res 2007;12:15–21.

[24] Makinde O. Similarity solution of hydromagnetic heat and mass transfer over a vertical plate with a convective surface boundary condition. Int J Phys Sci 2010;5:700–710.

[25] Groşan T, Sheremet MA, Pop I, Pop SR. Double-diffusive natural convection in a differentially heated wavy cavity under thermophoresis effect. J Thermophys Heat Transf 2018;32:1045–1058. [CrossRef]

[26] Sheremet M. The influence of cross effects on the characteristics of heat and mass transfer in the conditions of conjugate natural convection. J Eng Thermophysics 2010;19:119–127. [CrossRef]

[27] Yildiz S, Başaran B. Investigation of natural convection heat transfer along a uniformly heated vertical plate. Arab J Sci Eng 2019;44:1685–1696. [CrossRef]

[28] Acharya N. On the flow patterns and thermal control of radiative natural convective hybrid nanofluid flow inside a square enclosure having various shaped multiple heated obstacles. Eur Phys J Plus 2021;136:1–29. [CrossRef]

[29] Akinshilo A. Investigation of Lorentz force effect on steady nanofluid flow and heat transfer through parallel plates. J Therm Eng 2019;5:482–497. [CrossRef]

[30] Ekiciler R. CFD analysis of laminar forced convective heat transfer for TiO2/water nanofluid in a semi-circular cross-sectioned micro-channel. J Therm Eng 2021;5:123–137. [CrossRef]

[31] Rao M, Gangadhar K, Chamkha AJ, Surekha P. Bioconvection in a convectional nanofluid flow containing gyrotactic microorganisms over an isothermal vertical cone embedded in a porous surface with chemical reactive species. Arab J Sci Eng 2021;46:2493–2503. [CrossRef]

[32] Taskesen E, Tekir M, Gedik E, Arslan K. Numerical investigation of laminar forced convection and entropy generation of Fe3O4/water nanofluids in different cross-sectioned channel geometries. J Therm Eng 2021;7:1752–1767. [CrossRef]

[33] Rana S, Dura HB, Bhattrai S, Shrestha, R. Impact of baffle on forced convection heat transfer of CuO/water nanofluid in a micro-scale backward facing step channel. J Therm Eng 2022;8:310–322. [CrossRef]

[34] White F, Corfield I. Viscous Fluid Flow, vol. 3 New York: McGraw-Hill; 2006.